Absolute instruments and perfect imaging in geometrical optics

Tomáš Tyc, Lenka Herzánová,
Martin Šarbort and Klaus Bering
Institute of Theoretical Physics and Astrophysics,
Masaryk University, Kotlářská 2, 61137 Brno, Czech Republic

28 June 2011

Abstract

We investigate imaging by spherically symmetric absolute instruments that provide perfect imaging in the sense of geometrical optics. We derive a number of properties of such devices, present a general method for designing them and use this method to propose several new absolute instruments, in particular a lens providing a stigmatic image of an optically homogeneous region and having a moderate refractive index range.

1 Introduction

In the last decade, perfect imaging has become one of the hot topics in optics. This was triggered by a discovery of Sir J. Pendry [1] who showed that a slab of material with negative refractive index can focus light to a spot much smaller than the wavelength of light. Modern metamaterials with carefully designed electric and magnetic responses [2] provided a suitable experimental background for testing such super-resolution [3], but it has turned out that there are severe limitations due to a strong absorption in negatively refracting materials [4]. This started a search for other devices that could provide super-resolution but would not suffer from the disadvantages related to negative refraction. It has turned out recently that such devices do exist, which was demonstrated both theoretically [5, 6] and experimentally [7] for a well-known optical device, Maxwell's fish eye [8]. Optical imaging with super-resolution is generally called perfect imaging and the corresponding devices are called perfect lenses.

The concept of perfect imaging has become important also in geometrical optics where limitations of optical instruments are of a different kind. There, the diffraction limit of resolution is not the subject of investigation, but instead one seeks to minimise or even eliminate the optical aberrations of the device. Remarkably, there exist devices in which this elimination can be made perfect; they are called absolute instruments [9]. An important subset of absolute instruments is formed by devices that produce images geometrically similar to the imaged objects. Within geometrical optics, such images are called perfect [9]. Hence the meaning of "perfect imaging" is different in geometrical and in wave optics. In particular, an imaging device that is perfect from the point of view of geometrical optics may or may not be perfect from the point of view of wave optics, and vice versa. The only devices that are known to produce images perfect in both senses are Pendry's slab [1] and Maxwell's fisheye surrounded by a mirror [5, 7]; it remains unknown whether other lenses producing stigmatic

images also provide super-resolution. However, as the answer is very likely to be positive, a search for new absolute instruments with interesting and useful properties is highly desirable because such devices might provide unprecedented resolution and find applications in imaging or lithography.

In this paper, we focus on absolute instruments and perfect imaging from the point of view of geometrical optics. We analyse general properties of imaging by spherically symmetric absolute instruments and develop a method for designing such devices. We then use this method for proposing several devices with interesting properties.

The paper is organised as follows. In Sec. 2 we analyse spherically symmetric absolute instruments and derive several general results. In Sec. 3 we solve the inverse scattering problem for spatially confined rays and based on this result we develop a method for designing absolute instruments in Sec. 4. In Sec. 5 we give some simple examples of absolute instruments and in Secs. 6 and 7 we discuss devices with homogeneous regions and multiple image points, respectively. We conclude in Sec. 8.

2 Properties of spherically symmetric absolute instruments

In this paper we will consider isotropic spherically symmetric refractive index profiles $n(r)$. Such situations have a great advantage: if some point at radius r is imaged stigmatically, then the same is true for all points at the same radius. At the same time, usually the object to be imaged must be embedded directly into the optical medium and the rays emerge in all directions from the object and come from all directions to the image. This is quite different from the usual imaging e.g. by a camera or a telescope where rays propagate more or less in one direction.

2.1 Angular momentum and turning parameter

It is well known (and follows for example from the analogy between geometrical optics and classical mechanics) that in spherically symmetrical refractive index profiles $n(r)$ light rays propagate in a plane containing the centre of symmetry. This is a consequence of conservation of the quantity analogous to mechanical angular momentum, the magnitude of which is [9]

$$L = rn(r)\sin\alpha\,, \tag{1}$$

where α is the angle between the tangent to the particle trajectory and the radius vector. Motion in spherically symmetric index distributions $n(r)$ is therefore effectively two-dimensional, and we will treat it as such unless otherwise stated.

For a spherically symmetric medium, an important role is played by the radially normalised index function

$$N(r) = rn(r)\,, \tag{2}$$

which is also known as the turning parameter [10, 11]. Consider a light ray propagating with angular momentum L. It follows from Eqs. (1) and (2) that $L = N(r)\sin\alpha$ and hence the ray can propagate only in the regions where $L \leq N(r)$. When it gets to the point where $L = N(r)$, then $\alpha = \pi/2$ and the ray propagates purely in the angular direction. Such a point is called a turning point.

2.2 Stigmatic images and absolute instruments

According to Principles of Optics by M. Born and E. Wolf [9], an absolute instrument is a device that images stigmatically a three-dimensional domain of space. A stigmatic image of a point A is a point B through which an infinity of rays emerging from A pass.

We shall distinguish between two cases of a stigmatic image. In the first case, the image of a point A is formed at B by all rays emerging from A into some nonzero solid angle. We shall then call B a *strong stigmatic image* (or simply *strong image*) of A. In the second case, although there is an infinite number of rays going from A to B, these rays constitute just a zero solid angle. Then we shall call B a *weak [stigmatic] image*. For example, a cylindrical lens can form a whole line of weak images of a given point but no strong image.

2.3 Mutual position of an object and its image

Suppose we have an absolute instrument with refractive index $n(r)$ that stigmatically images a point A with radial coordinate r_A to a point B with radial coordinate r_B. This means that an infinite number of rays emerging from A meet at B [9]. Imagine we shift the point A infinitesimally in the angular direction by an angle $\mathrm{d}\varphi$ to a new position A′ separated from A by distance $r_\mathrm{A}\mathrm{d}\varphi$. From the spherical symmetry it follows that the image B gets shifted by the same angle $\mathrm{d}\varphi$ to a new position B′ separated from B by $r_\mathrm{B}\mathrm{d}\varphi$. Now Maxwell's theorem for absolute instruments [9] states that the optical length of any curve and of its image is the same, which we can apply to the lines AA′ and BB′. Cancelling the angle $\mathrm{d}\varphi$, we obtain

$$n(r_\mathrm{A})\, r_\mathrm{A} = n(r_\mathrm{B})\, r_\mathrm{B}\,. \tag{3}$$

Assuming that we shift the point A in the radial direction by $|\mathrm{d}r_\mathrm{A}|$ to a point A″ instead, the point B is shifted also in the radial direction to the point B″. This follows from the fact that imaging by absolute instruments is conformal [9], another consequence of Maxwell's theorem: if the angle A′AA″ is $\pi/2$, so must be the angle B′BB″. From Maxwell's theorem applied to the lines AA″ and BB″ we then get

$$n(r_\mathrm{A})|\mathrm{d}r_\mathrm{A}| = n(r_\mathrm{B})|\mathrm{d}r_\mathrm{B}|\,. \tag{4}$$

Dividing Eq. (4) by Eq. (3), we get

$$\frac{\mathrm{d}r_\mathrm{A}}{r_\mathrm{A}} = \pm\frac{\mathrm{d}r_\mathrm{B}}{r_\mathrm{B}} \tag{5}$$

with the solutions

$$r_\mathrm{B} = k r_\mathrm{A} \tag{6}$$

$$r_\mathrm{B} = \frac{k}{r_\mathrm{A}} \tag{7}$$

corresponding to plus and minus sign in Eq. (5), respectively, and an integration constant $k > 0$.

Another question is related to the mutual angular position of an object and its image. Can there be a situation that the object A, its strong stigmatic image B and the origin O (centre of symmetry of the lens) do not lie on a single straight line? Imagine such a situation. Since B is a strong image of A, a full solid angle of rays starting from A pass through B. We can rotate these rays around the line OA by some angle φ, which also moves the point B to a new position B′. The rotated rays now pass through B′ which, due to the spherical symmetry of the lens, must also be a strong stigmatic image of A. This would mean that A has strong images along the whole circle that is obtained by rotation of the point B around the axis OA, which is clearly impossible. So we must conclude that the points A, B and O lie on a single straight line. This way the image B is either on the exactly same side from O as is A or on the exactly opposite side.

Note that this argument is not valid in two dimensions where the mutual position of a point and its image in a rotationally-symmetric absolute instrument is less restricted. For the same reason this argument is not valid in 3D for weak images.

2.4 Value of the constant k in Eq. (6)

An interesting question is related to the possible values of the constant k in Eq. (6). We conjecture that the only possibility is $k = 1$. Although we have not been able to show this in the completely general situation, the proof can be given in two practically important cases. For the first case, assume that the constant k is the same for all the points that are imaged by the lens. But if B is an image of A, then also A is an image of B, so $r_{\mathrm{A}} = kr_{\mathrm{B}}$ must also hold along with Eq. (6), from which then $k = 1$ follows.

The assumption of the second case is that among the rays that contribute to the image B of a point A there is also the ray for which A is a turning point. In other words, we assume that a ray starting from the point A in the angular direction makes it to the image of A formed at the point B. Since Eq. (3) can be rewritten as $N(r_{\mathrm{A}}) = N(r_{\mathrm{B}})$, it follows that the point B is a turning point for the same ray as well. Next we use Eq. (5) with the plus sign from which Eq. (6) has been derived, i.e., $\mathrm{d}r_{\mathrm{A}}/r_{\mathrm{A}} = \mathrm{d}r_{\mathrm{B}}/r_{\mathrm{B}}$. From this equation combined with $N(r_{\mathrm{A}}) = N(r_{\mathrm{B}})$ then follows

$$r_{\mathrm{A}} \frac{\mathrm{d}N(r_{\mathrm{A}})}{\mathrm{d}r_{\mathrm{A}}} = r_{\mathrm{B}} \frac{\mathrm{d}N(r_{\mathrm{B}})}{\mathrm{d}r_{\mathrm{B}}} \,. \tag{8}$$

We see that the derivative $\mathrm{d}N/\mathrm{d}r$ has the same sign at both r_{A} and r_{B}. However, if $k \neq 1$, this is a contradiction with the fact that the same ray has its turning points at A as well as B. To see this, suppose that $k > 1$ (in the opposite case we can relabel the points A and B), so $r_{\mathrm{B}} > r_{\mathrm{A}}$. Then if the derivative $\mathrm{d}N/\mathrm{d}r$ is negative at $r = r_{\mathrm{A}}$, then for the ray with angular momentum $L = N(r_{\mathrm{A}})$ the region $r > r_{\mathrm{A}}$ is inaccessible because in this region $L > N(r)$, which is impossible, and so the ray cannot make it to B. On the other hand, if the derivative $\mathrm{d}N/\mathrm{d}r$ is positive at $r = r_{\mathrm{A}}$, then it is also positive at $r = r_{\mathrm{B}}$. For a similar reason then the ray with angular momentum $L = N(r_{\mathrm{A}}) = N(r_{\mathrm{B}})$ cannot make it to A, which is a contradiction. Hence the only possibility is $r_{\mathrm{A}} = r_{\mathrm{B}}$ which then implies $k = 1$.

We thus see that there are just two cases of imaging by spherically symmetric absolute instruments: either the image is given by spherical inversion (since $r_{\mathrm{A}}r_{\mathrm{B}} = k$) of the object, possibly combined with some rotation, or it is congruent with it. We have arrived at a slightly stronger statement than derived in [9] for absolute instruments in general. We will see in Sec. 4 that Eq. (7) corresponds to the generalised Maxwell's fish eye; all other spherically symmetric absolute instruments correspond to Eq. (6) with $k = 1$, so they give images congruent with the object and their magnification is unity. This means that the imaging by such a device is perfect in the sense of geometrical optics [9].

3 Inverse scattering problem for spatially confined rays

In the inverse scattering problem in mechanics, the task is to determine an unknown potential from the scattering angle which is a known (e.g. measured) function of the impact parameter. The problem was solved for central potentials in 1953 by O. B. Firsov [12] and the analogous problem in optics was solved by K. Luneburg [13]. In the situations considered there, the particle or light ray incides from infinity, undergoes scattering and leaves for infinity again, so the motion is not spatially confined. However, the situation where the motion is restricted to a finite region of space may be equally important for design of absolute instruments and perfect lenses. The inverse problem can be formulated and solved also in this case; the solution for mechanical motion was given without derivation by V. N. Ostrovsky in [14]. In the following we derive the inversion formula for confined motion in the optical case.

To derive the inversion formula, we will assume that the function $N : r \mapsto N(r)$ in Eq. (2) is increasing for $r \le r_0$ and decreasing for $r \ge r_0$ with some radius $r_0 > 0$. (There are obviously more general profiles $N(r)$ and the inverse problem can be solved for them as well, but we will not consider them here.) Then the function $N(r)$ has a global maximum $L_0 \equiv \max N = N(r_0)$ at the point $r = r_0$. The inverse function $r : N \mapsto r(N)$ is multi-valued, i.e., has two branches $r_\pm$. One branch $r_- : N \mapsto r_-(N)$ maps into the inner region $[0, r_0]$, and the other branch $r_+ : N \mapsto r_+(N)$ maps into the outer region $[r_0, \infty)$. In this case we can invert the inequality $L \le N(r)$ into a double inequality

$$r_-(L) \le r \le r_+(L)\,, \tag{9}$$

which explicitly specifies the allowed confined region. In other words, for angular momentum $L < L_0$, there are two turning points $r_\pm(L)$. Moreover, a light ray with angular momentum $L = L_0$ will propagate along a circular trajectory with radius r_0, while angular momentum $L > L_0$ is forbidden.

For the subsequent calculations, it turns out to be more convenient to work in terms of a new coordinate $x = \ln r$ rather than the radius r. We will also introduce corresponding notation $x_\pm = \ln r_\pm$, $x_0 = \ln r_0$, etc., in the obvious fashion. At a general point of a ray trajectory, the derivative of the polar angle φ is

$$\frac{\mathrm{d}\varphi}{\mathrm{d}x} = r\frac{\mathrm{d}\varphi}{\mathrm{d}r} = \tan\alpha = \frac{L}{\sqrt{N^2(r) - L^2}}\,, \tag{10}$$

where we have used that $L = N(r)\sin\alpha$. With the help of Eq. (10), the increment of the polar angle corresponding to motion between $r_-(L)$ and $r_+(L)$ can be written as

$$\Delta\varphi(L) = L\int_{r_-(L)}^{r_+(L)} \frac{\mathrm{d}r}{r\sqrt{N^2(r) - L^2}} = L\int_{x_-(L)}^{x_+(L)} \frac{\mathrm{d}x}{\sqrt{N^2(x) - L^2}}\,. \tag{11}$$

We shall call $\Delta\varphi$ the turning angle; it expresses the change of the ray direction between two consequent turning points.

The task of the inverse scattering problem is to find the refractive index $n(r)$ [or equivalently, the function $N(x)$] from the known turning angle $\Delta\varphi(L)$. It can be solved in a similar way to finding the 1D potential from the known period of oscillations as a function of energy [15]. We divide $\Delta\varphi(L')$ by $\sqrt{L'^2 - L^2}$, where L' is an integration parameter, and integrate with respect to L' from L to L_0:

$$\begin{aligned}
\int_L^{L_0} \frac{\Delta\varphi(L')\,\mathrm{d}L'}{\sqrt{L'^2 - L^2}} &\overset{(11)}{=} \int_L^{L_0}\int_{x_-(L')}^{x_+(L')} \frac{\mathrm{d}x}{\sqrt{N^2(x) - L'^2}}\frac{L'\,\mathrm{d}L'}{\sqrt{L'^2 - L^2}} \\
&= \int_{x_-(L)}^{x_+(L)}\int_L^{N(x)} \frac{L'\,\mathrm{d}L'}{\sqrt{L'^2 - L^2}}\frac{\mathrm{d}x}{\sqrt{N^2(x) - L'^2}} \\
&= \int_{x_-(L)}^{x_+(L)} \left[\arcsin\sqrt{\frac{L'^2 - L^2}{N^2(x) - L^2}}\right]_{L'=L}^{L'=N(x)} \mathrm{d}x \\
&= \int_{x_-(L)}^{x_+(L)} \left(\frac{\pi}{2} - 0\right)\mathrm{d}x = \frac{\pi}{2}\left(x_+(L) - x_-(L)\right)\,,
\end{aligned} \tag{12}$$

where we have inverted the order of integration and changed the integration limits appropriately, see Fig. 1. Equation (12) yields the inversion formula

$$\ln\frac{r_+(L)}{r_-(L)} = \frac{2}{\pi}\int_L^{L_0} \frac{\Delta\varphi(L')\,\mathrm{d}L'}{\sqrt{L'^2 - L^2}}\,, \tag{13}$$

which solves the inverse scattering problem. The mechanical equivalent of Eq. (13) was presented in [14] without derivation.

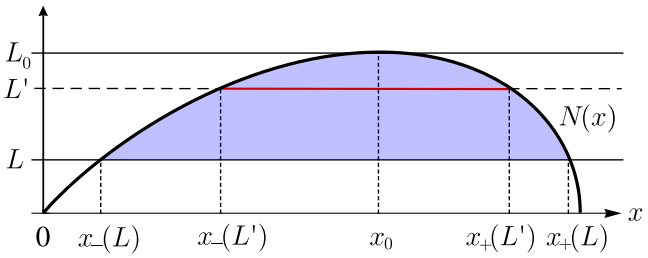

Figure 1: The change of integration limits in Eq. (12) illustrating that $\int_L^{L_0}\int_{x_-(L')}^{x_+(L')} u(x,L')\,\mathrm{d}x\,\mathrm{d}L' = \int_{x_-(L)}^{x_+(L)}\int_L^{N(x)} u(x,L')\,\mathrm{d}L'\,\mathrm{d}x$.

4 Method for designing absolute instruments

In the following we will describe a general method for designing absolute instruments. This method was sketched in [14] but was not given explicitly.

Consider the situation when the turning angle $\Delta\varphi$ is independent of L and equal to π/m, $m \in \mathbb{R}$. This is a practically important case; if, for instance, $m = p/q$ with p, q coprimes and p even, then the trajectory will be symmetric with respect to rotation by π around the origin in the plane of propagation. A strong stigmatic image of a point A at the position $\vec{r}$ will therefore be formed at $-\vec{r}$. If $m = p/q$ with p odd, a strong stigmatic image of a point A will be formed at A itself; the ray arrives there after encircling the origin q times. This will be shown in Fig. 5.

For $\Delta\varphi(L) = \pi/m$ we get from Eq. (13) $\ln[r_+(L)/r_-(L)] = (2/m)\,\mathrm{arcosh}\,(L_0/L)$, which can be expressed as

$$\frac{L_0}{L} = \frac{1}{2}\left[\left(\frac{r_+(L)}{r_-(L)}\right)^{m/2} + \left(\frac{r_-(L)}{r_+(L)}\right)^{m/2}\right]. \tag{14}$$

Now comes the key step of our derivation. We define a function $f(r)$ such that

$$f(r) = \begin{cases} r_+(N(r)) & \text{for} \quad r \le r_0 \\ r_-(N(r)) & \text{for} \quad r \ge r_0\,. \end{cases} \tag{15}$$

The function $f(r)$ is hence defined such that for a given lower turning point r_- it produces the upper turning point r_+ corresponding to the same angular momentum and vice versa:

$$r_\pm = f(r_\mp)\,. \tag{16}$$

We can say that the point r_+ is dual to the point r_- and vice versa. It also follows from this definition that applying the function f twice yields the original value, $f(f(r)) = r$, and therefore the graph of f is symmetric with respect to the axis of the first quadrant. The graph intersects this axis at the point $r_+ = r_- = r_0$, which corresponds to the circular ray trajectory.

With the function $f(r)$ defined this way, we can express L from Eq. (14) and either keep r_- and replace r_+ by $f(r_-)$, or keep r_+ and replace r_- by $f(r_+)$. Taking then advantage of the fact that $L = N$ at $r_\pm$ and omitting the index of $r_\pm$, we get

$$N(r) = 2L_0\left[\left(\frac{r}{f(r)}\right)^{m/2} + \left(\frac{f(r)}{r}\right)^{m/2}\right]^{-1}. \tag{17}$$

Finally we express $n(r) = N(r)/r$ as

$$n(r) = \frac{2L_0}{r\left[\left(\frac{r}{f(r)}\right)^{m/2} + \left(\frac{f(r)}{r}\right)^{m/2}\right]}\,. \tag{18}$$

Equation (18) provides a powerful tool for designing absolute instruments. For any chosen function $f(r)$ satisfying the condition above and a suitable value of m it gives a refractive index profile with focusing properties, i.e., an absolute instrument. We will demonstrate this on several known examples first and then proceed to new devices.

5 Examples of absolute instruments

In all the following examples we assign unit radius and unit refractive index to the circular ray, so $r_0 = L_0 = 1$. In the first example the object and its image are related by spherical inversion, in the other ones they are congruent, as discussed in Sec. 2.

- *Generalised Maxwell's fish eye*

  Consider an absolute instrument in which the position of object and image is given by Eq. (7). Apparently, if $r_{\rm A}$ is a turning point, then $r_{\rm B}$ must also be a turning point, which leads to $r_+ r_- = k = r_0^2 = 1$ (the case of a general k can be obtained easily by spatial scaling) and hence $f(r) = 1/r$. Then Eq. (18) yields

  $$n(r) = \frac{2}{r^{1-m} + r^{m+1}}\,, \tag{19}$$

  which is the generalised Maxwell's fish eye profile discussed in [16]. Light rays in this lens are shown in Fig. 2 (a) for $m = 1/2$.

  For $m = 1$ we get

  $$n(r) = \frac{2}{1 + r^2}\,, \tag{20}$$

  which is the well-known Maxwell's fish eye refractive index profile [8]. The trajectories are circles intersecting the unit circle at two opposite points. Light rays are shown in Fig. 2 (b).

- *Luneburg lens profile*

  Take $m = 2$ and $f(r) = \sqrt{2 - r^2}$. Then Eq. (18) yields

  $$n(r) = \sqrt{2 - r^2}\,. \tag{21}$$

  For $r \le 1$ this coincides with the well-known refractive index of Luneburg lens [13] which has, however, $n = 1$ for $r > 1$. The index (21) corresponds to Hooke potential in mechanics and ray trajectories are ellipses centred at the origin [11], see Fig. 3 (a).

- *Eaton/Miñano lens profile*

  Take $m = 1$ and $f(r) = 2 - r$. Then Eq. (18) yields

  $$n(r) = \sqrt{(2/r) - 1}\,. \tag{22}$$

  This is the well-known index profile of Eaton or Miñano lens [17, 18] which have, however, $n = 1$ for $r > 1$ or $r < 1$, respectively. The index (22) corresponds to elliptic motion in Newton potential in mechanics and ray trajectories are confocal ellipses with focus at the origin and with the main semiaxes of unit length [11], see Fig. 3 (b).

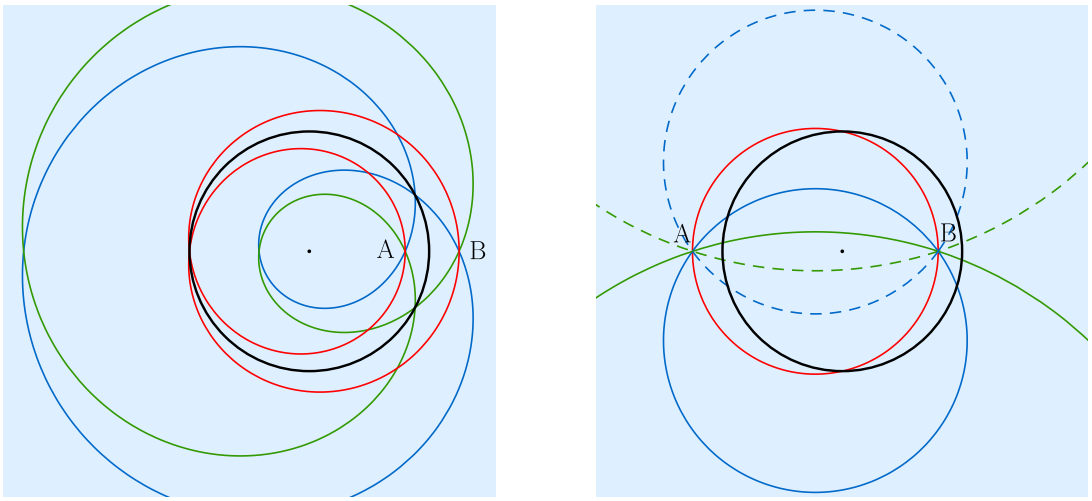

(a) (b)

Figure 2: Ray trajectories in (a) generalised Maxwell's fish eye with $m = 1/2$ and (b) Maxwell's fish eye. The source and its image are denoted by A and B, respectively. Here as well as in all subsequent figures, the black circle corresponds to the circular trajectory at $r = r_0$ with the maximum possible angular momentum L_0.

- *Maxwell's fish eye mirror*

  Take $m = 2$ and $f(r) = 1$ for $r < 1 = r_0$. From the symmetry of the function f it follows that it is undefined for $r \geq 1$; the rays cannot get beyond the unit circle, which means they must be reflected there. Substituting into Eq. (18), we get for $r \in [0, 1)$ the index given by Eq. (20). This is the so-called Maxwell's fish eye mirror discussed in detail in [5] with rays shown in Fig. 4.

- *Lenses generated by a sample function $f(r)$*

  To show the generality of our method, we choose some arbitrary function $f(r)$ with the restriction that it is symmetric with respect to the axis of the first quadrant. Let us choose

$$f(r) = \begin{cases} 3 - 2r & \text{for} \quad r \leq 1 \\ (3 - r)/2 & \text{for} \quad r \geq 1 \end{cases} \tag{23}$$

  see its graph in Fig. 5 (a). Using different values of m, we get different absolute instruments. The rays in some of them are shown in Fig. 5 (b) – (d) for $m = 2$, $m = 5/2$ and $m = 2/3$.

5.1 Lenses with mirrors and index discontinuities

On the example of Maxwell's fish eye mirror we have seen that an interval of r on which the function $f(r)$ from Eq. (16) was constant corresponded to a spherical mirror. As we will see, this is quite a general feature.

Consider the situation when the function $f(r)$ is constant and equal to $c \geq r_0$ on some interval (a, b) with $b \leq r_0$. In other words, the upper turning point is the same for different lower turning points and hence for different angular momenta; the corresponding rays cannot get beyond $r = c$, which means there occurs reflection at this point. Now there are two cases to be distinguished. In

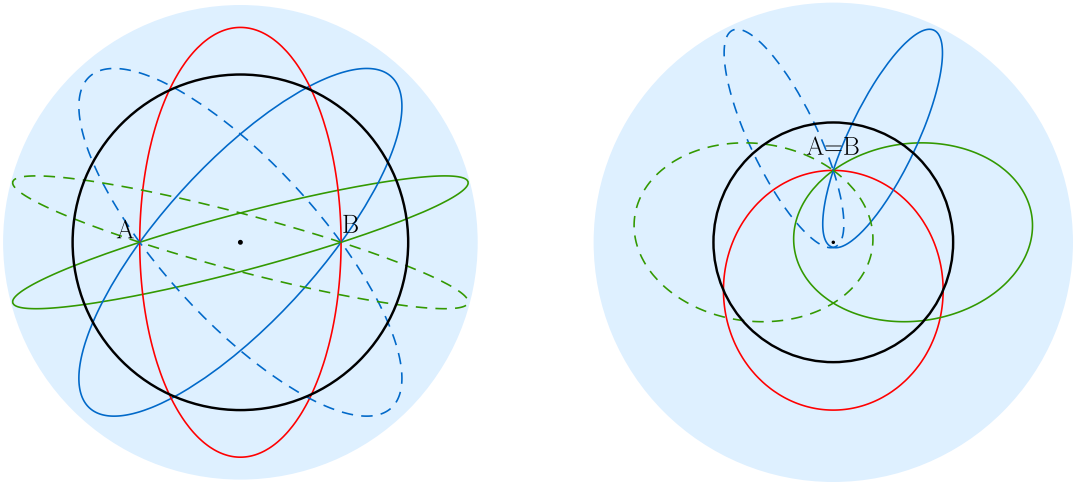

(a) (b)

Figure 3: Ray trajectories in the profile given by (a) Eq. (21) corresponding to Luneburg profile and (b) Eq. (22) corresponding to Eaton/Miñano profile. The optical medium is shown in light blue colour; the refractive index goes to zero at the edge of the medium. In Eaton/Miñano profile the image B coincides with the source A.

the first case $f(r) = c$ holds also for $0 \leq r < a$, which means that a reflection occurs for all rays that reach the point $r = c$; this corresponds to a perfect mirror placed at c. In the second case, the value $f(r)$ gets larger than c for some $r < a$. This means that rays with small angular momenta can penetrate beyond c; the reflection at c mentioned above must then be total internal reflection caused by a refractive index discontinuity at $r = c$. That such a discontinuity indeed exists follows from the fact that if $f(r) = c$ on the interval (a, b), then $f(r)$ must be discontinuous at $r = c$ and so must be $n(r)$ according to Eq. (18).

If the interval of constant f lies above r_0 then there will be a total reflection on a sphere "from the outside". This is illustrated in Fig. 6 where there is a mirror reflecting perfectly from the inside and a jump of refractive index reflecting totally some rays from the outside.

Spherical mirrors can be used with a great advantage to reduce the size of the lens and also the range of the refractive index. An example is Maxwell's fish eye mirror discussed above that has equally good focusing properties as the original Maxwell's fish eye but its size is reduced from infinity to a unit disc (or sphere) and the refractive index range is reduced significantly from the interval $(0, 2]$ to just $[1, 2]$.

6 Absolute instruments for homogeneous regions

In many absolute instruments such as Maxwell's fish eye, the optical medium fills the whole space and the object to be imaged must therefore be inserted into such an inhomogeneous medium. It is desirable to find optical devices that provide images of optically homogeneous spatial regions, i.e., regions with a uniform refractive index. Even if the refractive index of such a region differs from unity, this is still an advantage because one can fill this region with a suitable liquid and place the object in it.

Interestingly, until recently the only known devices providing stigmatic images of optically homogeneous 3D regions were plane mirrors or their combinations [9]. This has changed by an excellent

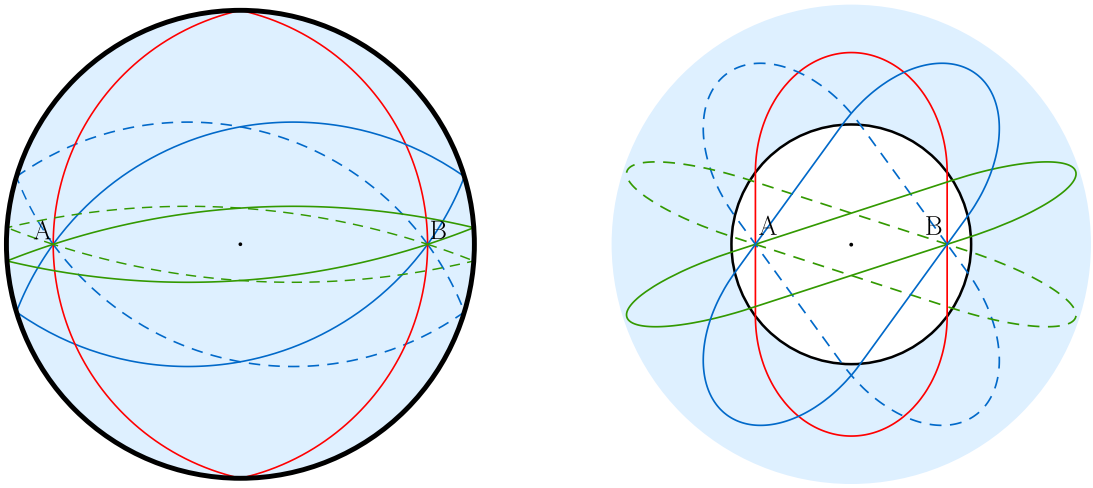

(a) (b)

Figure 4: Ray trajectories in (a) Maxwell's fish eye mirror an (b) Miñano lens. Optically homogeneous region is shown in white colour.

work of J. C. Miñano [18] who noticed that some well-known optical devices such as Eaton or Luneburg lens [13] are in fact absolute instruments, providing stigmatic virtual images. An even more important result of [18], however, is a a device now called Miñano lens that provides real images of homogeneous 3D regions.

6.1 Miñano lens

In Miñano lens the homogeneous region is the unit disc with unit refractive index and the turning angle is $\Delta\varphi = \pi/2$, which corresponds to $m = 2$. To derive the refractive index outside the unit disc by our method, we will again use Eq. (18), but first we have to determine the function f. The lower turning point for a given L is simply $r_- = L$ because $n = 1$ in this region, the upper turning point is $r_+ = f(r_-)$. Substituting this into Eq. (14), we get a quadratic equation $f^2(r_-) - 2f(r_-) + r_-^2 = 0$ for $f(r_-)$ with the solution

$$r_+ = f(r_-) = 1 + \sqrt{1 - r_-^2} \tag{24}$$

(we have taken the larger root so that $r_+ \geq r_-$). Inverting this expression to get the function f also for r_+, we find $r_- = f(r_+) = \sqrt{2r_+ - r_+^2}$. Now we can combine Eqs. (18) and (24) with $L_0 = 1$ to find the refractive index outside the unit disc. This gives precisely the expression (22), so the refractive index of Miñano lens is

$$n(r) = \begin{cases} 1 & \text{for} \quad r \leq 1 \\ \sqrt{(2/r) - 1} & \text{for} \quad r > 1 \end{cases} \tag{25}$$

and the ray trajectories are shown in Fig. 4 (b).

6.2 Modified Miñano lens

Despite its elegance and nice properties, Miñano lens has a disadvantage: its refractive index ranges from unity all the way to zero at $r = 2$, which is very difficult to realise practically. Since any

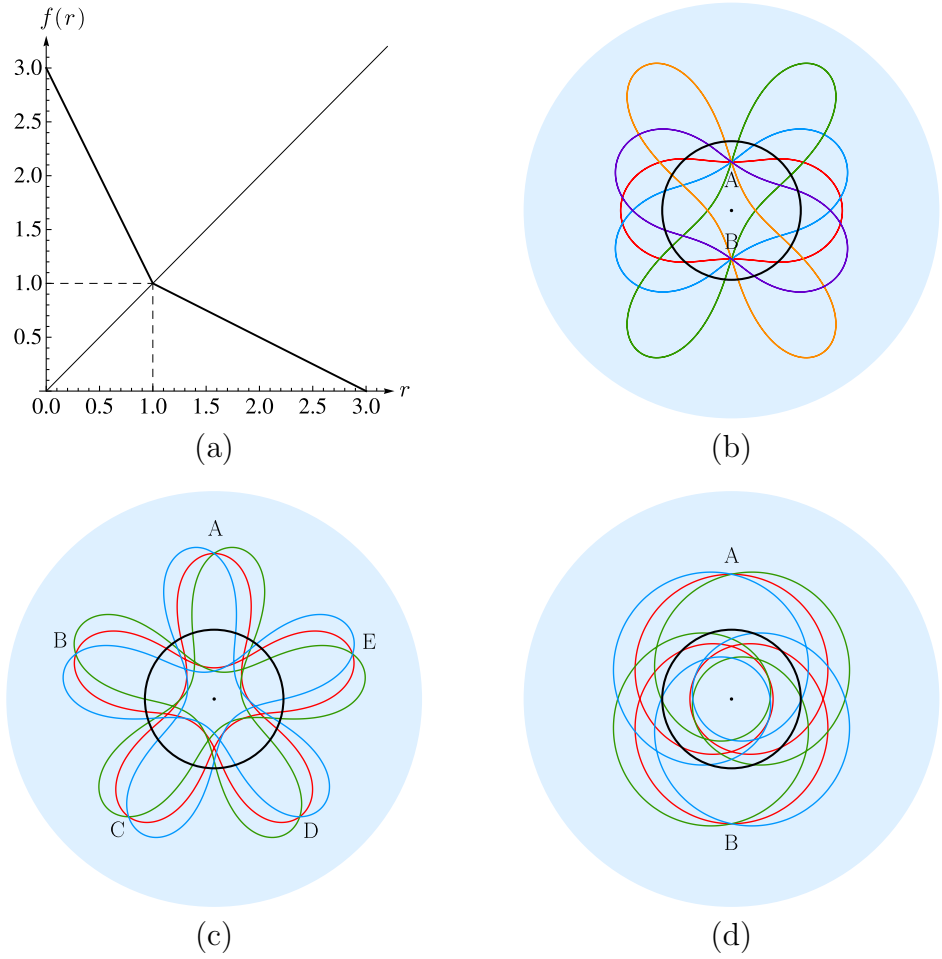

Figure 5: Graph of a sample function $f(r)$ according to Eq. (23) and the corresponding ray trajectories for (b) $m = 2$, (c) $m = 5/2$ and (d) $m = 2/3$. In (b) and (d), there is a strong image of A at B while in (c) the images B, C, D, E of A are just weak.

refractive index profile can be multiplied by a real number without affecting the lens performance, we can define a measure of the index range as the ratio of its largest and smallest value

$$\eta \equiv n_{\max}/n_{\min}\,. \tag{26}$$

For Miñano lens $\eta = \infty$. It would be very desirable to modify the lens somehow to make η finite. Fortunately, this is possible, as we will show now. Imagine we use the function f for $r < 1$ according to Eq. (24), but on the interval $[0, b]$ with $0 < b < 1$ we replace it by a constant value $c = 1+\sqrt{1-b^2}$. As we have seen, this corresponds to placing a mirror at $r = c$. The function f this way becomes

$$f(r) = \begin{cases} c & \text{for} \quad r \le b \\ 1 + \sqrt{1 - r^2} & \text{for} \quad b < r \le 1 \\ \sqrt{2r - r^2} & \text{for} \quad 1 < r \le c \end{cases} \tag{27}$$

see Fig. 7 (c), and refractive index

$$n(r) = \begin{cases} 2c/\left(r^2 + c^2\right) & \text{for} \quad r \le b \\ 1 & \text{for} \quad b < r \le 1 \\ \sqrt{2/r - 1} & \text{for} \quad 1 < r \le c \end{cases} \tag{28}$$

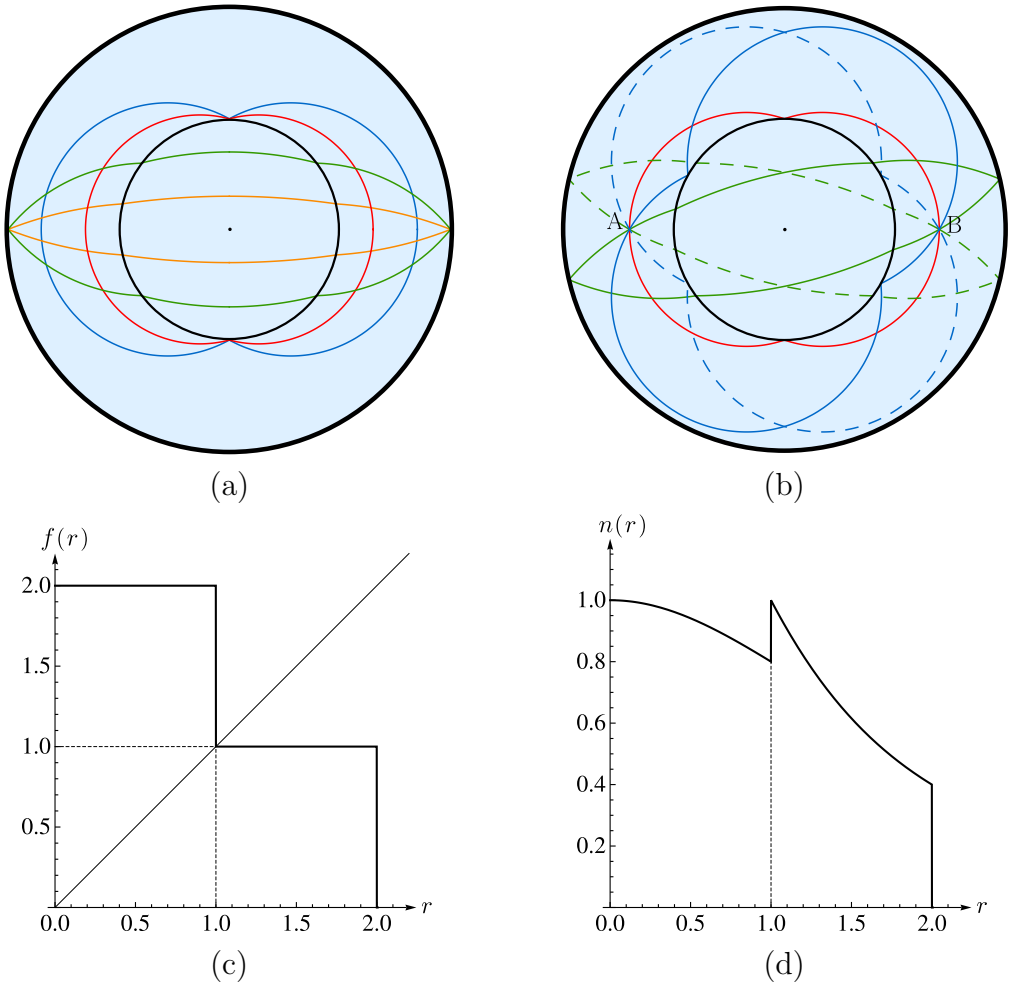

Figure 6: (a) Ray trajectories and (b) imaging by an absolute instrument with a spherical mirror at $r = 2$ and a jump of refractive index at radius $r = 1$. There are two types of ray trajectories differing by whether they do or do not penetrate inside the unit circle. (c) The corresponding function $f(r)$ and (d) refractive index.

see Fig. 7 (d). The largest and smallest values of the index occur at $r = 0$ and $r = c$, respectively, and yield the ratio $\eta = 2/b$. Choosing b not too small, one can get a very moderate index range of the lens; the price to pay is that the size of the homogeneous region is reduced. Rays in modified Miñano lens and its imaging properties are shown in Fig. 7 (a) – (b).

6.3 A lens for designing a magnifying absolute instrument

Recently we proposed another type of lens for imaging homogeneous spatial regions [19] that has a finite ratio of the largest and smallest refractive index. The homogeneous region is a unit sphere and there is a spherical mirror at radius $R > 1$. The refractive index between the two spheres is chosen such that a ray emerging in the direction of a unit vector $\vec{u}$ from a point A located at $\vec{r}_{\rm A}$ in the homogeneous region incides on the mirror at the point $R\vec{u}$. This ensures that the ray after the reflection from the mirror passes through the point B at $\vec{r}_{\rm B} = -\vec{r}_{\rm A}$ where an image of A is formed, see Fig. 8. Another property of the device is that, apparently, all mutually parallel rays propagating in the homogeneous region are focused to a single point at the mirror.

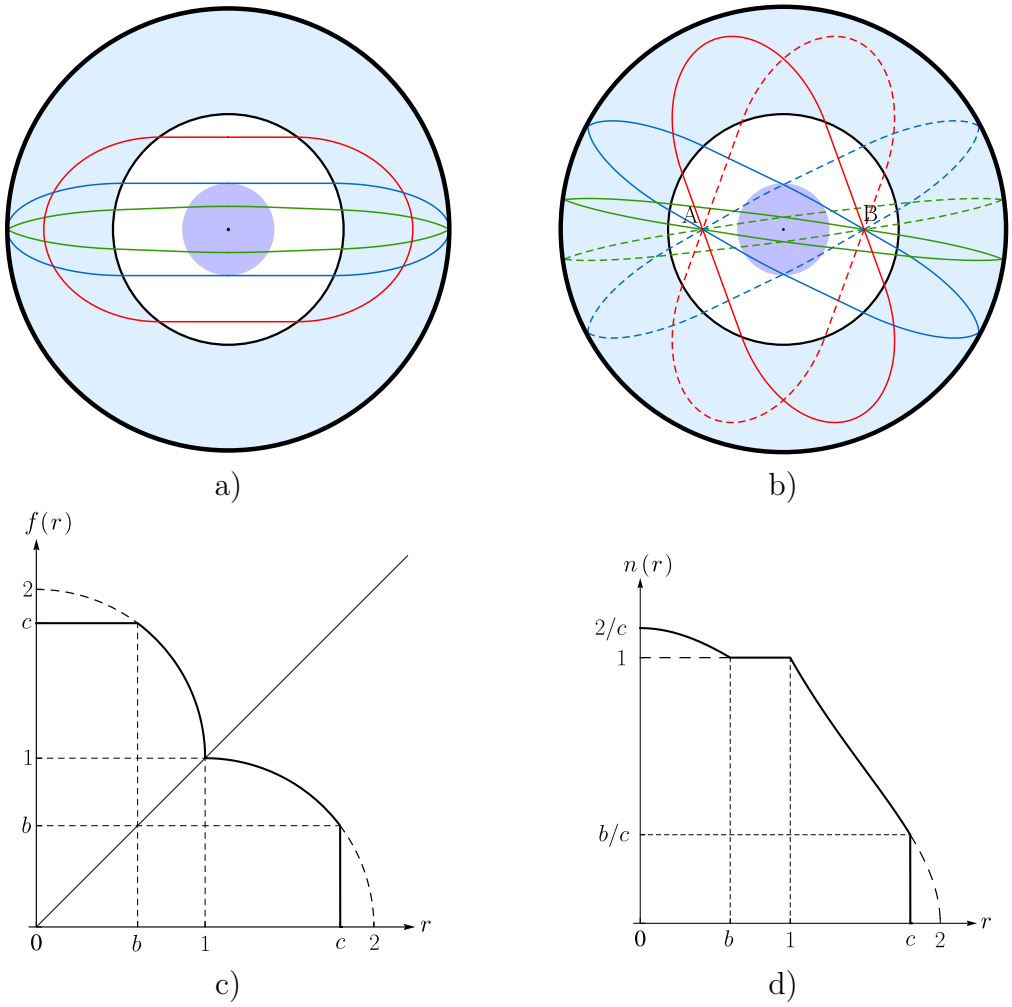

Figure 7: (a) Ray trajectories and (b) imaging by the modified Miñano lens. In contrast to Miñano lens, there is a spherical mirror at radius c and an inner inhomogeneous region of radius b. (c) The corresponding function $f(r)$ and (d) refractive index $n(r)$. The dashed parts of the graphs on the intervals $[0, b]$ and $[c, 2]$ correspond to the original Miñano lens.

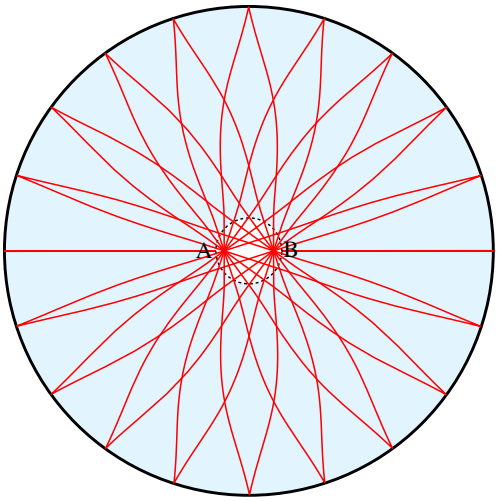

Figure 8: Rays in the lens imaging a circular homogeneous region employing a spherical mirror. The homogeneous region is encircled by a dotted line. Unfortunately, the refractive index performing such an imaging perfectly does not exist as we show in Appendix.

The refractive index calculated for this lens was based on numerical solution of a specific integral equation that does not have an analytic solution. Unfortunately, it has turned out later that the equation does not have solution at all, so the proposed lens is in fact not an absolute instrument. The rays emerging from A hence do not pass exactly through B but there is some unavoidable aberration. However, numerical simulations reveal that this aberration can be very small if R is not too small. For this reason the lens could have a practical importance, and we are therefore mentioning it here although it is not really an absolute instrument. The proof of non-existence of the solution of the integral equation is given in the Appendix.

7 Lenses with multiple image points

So far, we have considered just situations when the turning angle $\Delta\varphi(L)$ in Eq. (11) is constant for all angular momenta L from zero to L_0. However, another class of interesting absolute instruments can be obtained by taking $\Delta\varphi(L)$ piecewise constant on different intervals of L. In this situation, however, the refractive index cannot be found analytically with the help of Eq. (13) but must be calculated numerically. The simplest situation corresponds to two values of turning angle: $\Delta\varphi(L) = \pi/m_1$ for $L \in [0, L_1]$ and $\Delta\varphi(L) = \pi/m_2$ for $L \in [L_1, L_0]$. Fig. 9 (a) – (b) shows an example of this lens for $m_1 = 1$ and $m_2 = 2$. Rays emerging from the point A with angular momentum larger than L_1 meet first at the point B where they form an image and then continue back to A. On the other hand, rays with $L < L_1$ go back to A directly without passing through B. This way, the image B is formed just by some rays while the image A is formed by all rays.

Since there is not a smooth transition from the first class of rays (those with $L > L_1$) to the second class ($L < L_1$), the optical path from A to B does not have to be the same for rays of the two types. In other words, the principle of equal optical path [9] does not apply to this type of lens.

Another example of such a "bifocal lens" is shown in Fig. 9 (c) – (d) for $m_1 = 2$ and $m_2 = 4$. In the two-dimensional version of this problem, some rays emerging from A form an image at C or D and then continue to the image B. Other rays go to B directly without passing through C or D. If the lens is three-dimensional, a strong image will be just at B (and then at A again), but weak

images of A will be formed on the circle made by rotation of the points C and D about the axis AB. For coherent light waves emitted from the source at A, the inequality of the optical paths from A to B for the two ray types could lead to interesting diffraction patterns around the image point B if the two corresponding waves interfere destructively.

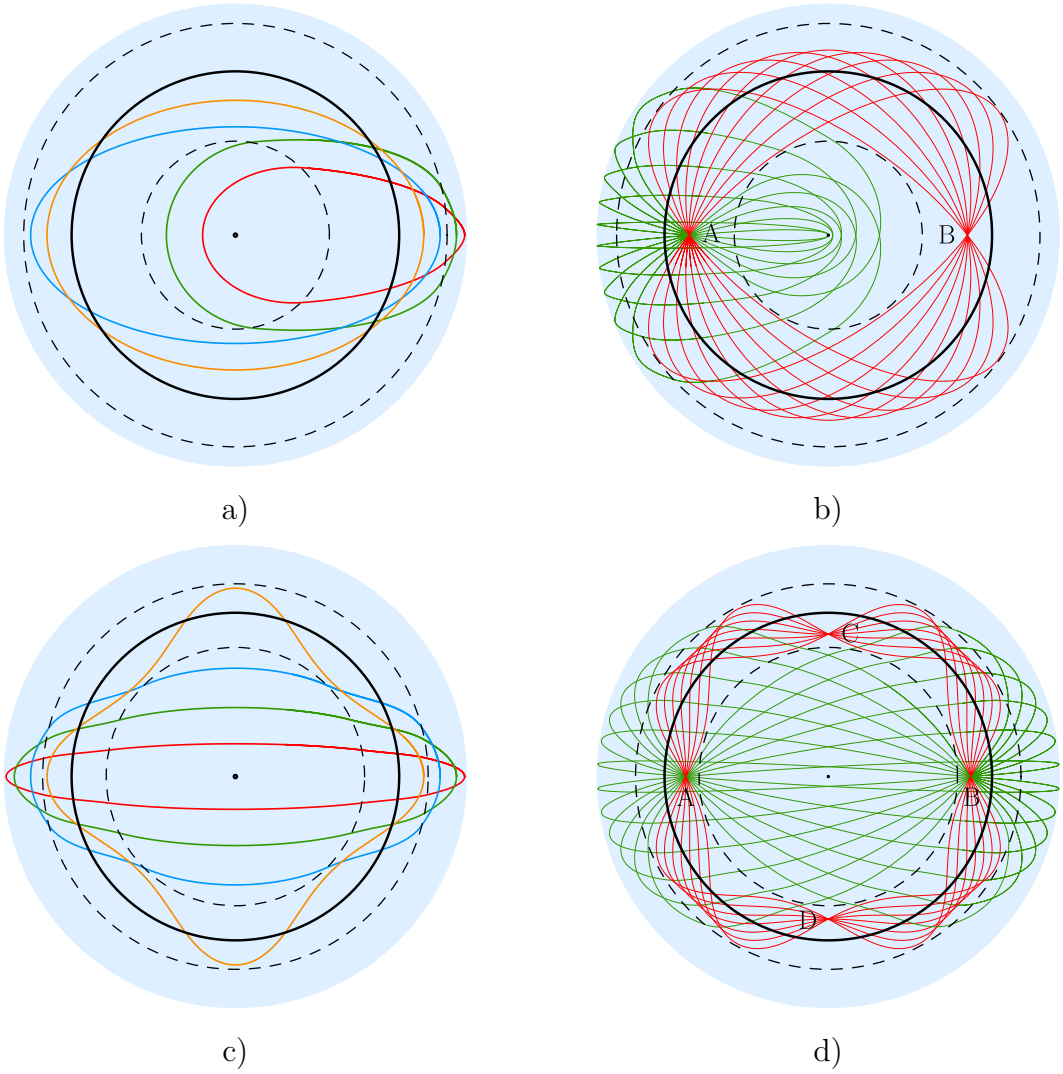

Figure 9: Ray trajectories in "bifocal" lens with $L_0 = 1, L_1 = 3/4$, $f(r) = \sqrt{2a^2 - r^2}$ and (a) – (b) $m_1 = 1$, $m_2 = 2$ and (c) – (d) $m_1 = 2$, $m_2 = 4$. The dashed circles mark the radii of turning points corresponding to angular momentum L_1. Rays confined to the ring between these circles have turning angle $\Delta\varphi = \pi/m_2$ while rays that get outside the ring have $\Delta\varphi = \pi/m_1$.

8 Conclusion

In this paper we have derived a number of results for imaging by spherically symmetric absolute instruments. We have shown that images created by such instruments are either congruent with the object or related to it by spherical inversion. We have also proved that the mutual position of a point and its strong image is quite restricted in 3D: the straight line connecting the two points must intersect the centre of the lens.

Further, we have developed a general method for designing absolute instruments via solving the inverse problem for finite motion. We have shown how this method can be used for designing already known as well as a number of new absolute instruments. The modified Miñano lens we have proposed is particularly appealing because it produces a real stigmatic image of a homogeneous region with a reasonable range of refractive index, and we believe that this lens can find important practical applications. Whether the imaging devices discussed in this paper can provide super-resolution remains an open question, but in our opinion the answer is positive.

Acknowledgements

This work was supported by the grants MSM0021622409 and MSM0021622419 of the Czech Ministry of Education and by GAČR 202/08/H072.

Appendix: No-Go Theorem for Spherically Symmetric Lenses

In the following we show that the refractive index with the appealing properties described in Sec. 6.3 does not exist. This gives a negative answer to the following question: is there a spherically symmetric medium that focuses parallel rays in a spherical cavity via a shell-shaped lens into a single point? If the answer were positive, this would constitute a new interesting and practically important absolute instrument as well as a useful building block for other optical devices [19]. Although the actual answer is negative by itself, it still useful and likely to influence future developments in the subject [20].

Consider parallel rays located in an inner spherical region $r \leq r_*$ with a constant refractive index $n_* \equiv \frac{N_*}{r_*} > 0$ that are focused by the medium to a point P situated at some finite distance $R > r_*$ from the centre O. We will try to determine an appropriate spherically symmetric profile $N(r) = rn(r)$ in the intermediate shell region

$$r_* \;\leq\; r \;\leq\; R \tag{29}$$

with inner and outer radius $r_* > 0$ and $R < \infty$, respectively. We will assume that all rays are outgoing, *i.e.*, the radial position of a light ray $r(t)$ is monotonically increasing as a function of time t, so no turning points are allowed. In particular, the outer region $r > R$ will play no role, and we might as well assume that the focal point P lies on the outer rim of the device. Suppose that the parallel rays move horizontally to the left and are focused to the focal point P with polar coordinates (R, π). As before, it is convenient to introduce the logarithm $x \equiv \ln r$ of the radial coordinate r. Similarly, we shall write $x_* \equiv \ln r_*$, $X \equiv \ln R$ etc. in an obvious notation.

Clearly N_* is the upper bound for the angular momentum L inside the inner region $r \leq r_*$. However, we shall only require that the focusing device actually works for rays with $L \in [0, L_m)$, where $L_m \in (0, N_*]$. A ray with angular momentum L emerges horizontally to the left from the inner rim at a polar angle $\pi - \arcsin \frac{L}{N_*}$ and when it arrives at P, the polar angle becomes π, so the corresponding change of polar angle is $\arcsin \frac{L}{N_*}$. On the other hand, the same change can be calculated by integrating Eq. (10) from r_* to R, so we arrive at the following integral equation:

$$\forall L \in [0, L_m): \quad \tfrac{1}{L} \arcsin \tfrac{L}{N_*} \;=\; \int_{r_*}^{R} \frac{\mathrm{d}r}{r\sqrt{N^2(r) - L^2}} \;\equiv\; \int_{x_*}^{X} \frac{\mathrm{d}x}{\sqrt{N^2(x) - L^2}} \;. \tag{30}$$

We next redefine (normalise) the quantities $N' := \frac{N}{N_*}$, $L' := \frac{L}{N_*}$, $L'_m := \frac{L_m}{N_*}$, etc., by dividing with the constant N_*. Suppressing the primes from now on, we arrive at the main integral equation [19],

$$\boxed{\forall L \in [0, L_m): \quad \frac{\arcsin(L)}{L} \;=\; \int_{r_*}^{R} \frac{\mathrm{d}r}{r\sqrt{N^2(r) - L^2}} \;\equiv\; \int_{x_*}^{X} \frac{\mathrm{d}x}{\sqrt{N^2(x) - L^2}} \;,} \tag{31}$$

which serves as our starting point. The solution function $N=N(r)$ is required to be bounded

$$\exists N_m \; \forall r \in [r_*, R]: \quad 0 < L_m \leq N(r) \leq N_m < \infty \tag{32}$$

for physical reasons, and Lebesgue measurable [21] in order for the integral (31) to be defined. Since the integrand (31) is non-negative, the integral is always defined, although perhaps infinite. The goal is now to investigate the integral equation (31), and show that it has no bounded solutions $N=N(r)$.

Note that the k'th moment $\int_{r_*}^{R} \frac{\mathrm{d}r}{r} \frac{1}{N^k(r)}$ is well-defined and finite for any integer k because of the bounds (29) and (32).

Lemma 8.1 (Reformulation in terms of odd moments) *The integral equation (31) is equivalent to*

$$\boxed{\int_{r_*}^{R} \tfrac{\mathrm{d}r}{r} \tfrac{1}{N^{2n+1}} \;=\; \tfrac{1}{2n+1} \quad \text{for} \quad n \in \mathbb{N}_0 \equiv \{0,1,2,3,\ldots\}\;.} \tag{33}$$

Proof: The Taylor expansion of the $\arcsin(L)$ function at $L=0$ is

$$\tfrac{\arcsin(L)}{L} \;=\; \textstyle\sum_{n=0}^{\infty} \frac{1}{2n+1} \left(\begin{array}{c} 2n \\ n \end{array} \right) \left(\frac{L}{2}\right)^{2n} \;. \tag{34}$$

On the right-hand side of Eq. (31), a binomial expansion produces

$$\begin{aligned} \int_{x_*}^{X} \tfrac{\mathrm{d}x}{\sqrt{N^2-L^2}} \;&=\; \int_{x_*}^{X} \tfrac{\mathrm{d}x}{N} \left(1-(\tfrac{L}{N})^2\right)^{-\frac{1}{2}} \;=\; \int_{x_*}^{X} \tfrac{\mathrm{d}x}{N} \textstyle\sum_{n=0}^{\infty} \left(\begin{array}{c} -\frac{1}{2} \\ n \end{array} \right) \left(-(\tfrac{L}{N})^2\right)^n \\ &=\; \int_{x_*}^{X} \tfrac{\mathrm{d}x}{N} \textstyle\sum_{n=0}^{\infty} \left(\begin{array}{c} 2n \\ n \end{array} \right) \left(\frac{L}{2N}\right)^{2n} \;=\; \textstyle\sum_{n=0}^{\infty} \left(\begin{array}{c} 2n \\ n \end{array} \right) \int_{x_*}^{X} \tfrac{\mathrm{d}x}{N} \left(\frac{L}{2N}\right)^{2n} \;. \end{aligned} \tag{35}$$

In the last equality of Eq. (35), we were allowed to exchange integration and summation order, because each term is positive or zero (Tonelli's Theorem). In the third equality of Eq. (35), we have used the identity

$$\left(\begin{array}{c} -\frac{1}{2} \\ n \end{array} \right) \;=\; \left(\begin{array}{c} 2n \\ n \end{array} \right) \left(-\tfrac{1}{4}\right)^n \;. \tag{36}$$

Comparing the Taylor-coefficients on the left-hand side (34) and right-hand side (35) of Eq. (31) yields the reformulation (33). $\square$

Lemma 8.2 (Reformulation in terms of new L) *The integral equation (31) is equivalent to*

$$\boxed{\forall L \in \mathbb{C}: \; e^{L^2} \;=\; \int_{r_*}^{R} \tfrac{\mathrm{d}r}{rN} \left(1+2(\tfrac{L}{N})^2\right) \exp\left[(\tfrac{L}{N})^2\right] \;\equiv\; \left(1+\tfrac{\mathrm{d}}{\mathrm{d}\alpha}\right) \int_{r_*}^{R} \tfrac{\mathrm{d}r}{rN} \exp\left[(\tfrac{\alpha L}{N})^2\right]\Big|_{\alpha=1} \;.} \tag{37}$$

Proof: The integrals in Eq. (37) are well-defined due to the bounds (29) and (32). We calculate

$$\begin{aligned} & L \textstyle\int_{x_*}^{X} \frac{\mathrm{d}x}{N} \exp\left[(\frac{L}{N})^2\right] \;=\; L \int_{x_*}^{X} \frac{\mathrm{d}x}{N} \sum_{n=0}^{\infty} \frac{1}{n!} \left(\frac{L}{N}\right)^{2n} \;=\; \sum_{n=0}^{\infty} \frac{1}{n!} \int_{x_*}^{X} \mathrm{d}x \left(\frac{L}{N}\right)^{2n+1} \\ \overset{(33)}{=}\; & \textstyle\sum_{n=0}^{\infty} \frac{1}{n!} \frac{L^{2n+1}}{2n+1} \;=\; \sum_{n=0}^{\infty} \frac{1}{n!} \int_0^L \mathrm{d}\ell \; \ell^{2n} \;=\; \int_0^L \mathrm{d}\ell \sum_{n=0}^{\infty} \frac{1}{n!} \ell^{2n} \;=\; \int_0^L \mathrm{d}\ell \; e^{\ell^2} \;. \end{aligned} \tag{38}$$

In the second equality of Eq. (38), we use Tonelli's and Fubini's Theorems [21] with x-independent majorant $\frac{|L|}{L_m} \exp\left[(\frac{|L|}{L_m})^2\right]$ to justify exchange of integration and summation order. Tonelli's and Fubini's Theorems are also used in the fifth equality of Eq. (38) with majorant $e^{|\ell|^2}$. Now differentiate both sides of Eq. (38) with respect to L to obtain Eq. (37). Note that Eq. (38) is trivially satisfied for $L=0$, so we do not lose information when differentiating. Therefore we can also run the argument backwards. $\square$

Thus we have three equivalent conditions, Eqs. (31), (33) and (37), that a solution $N=N(r)$ should satisfy.

Lemma 8.3 *If there exists a solution $N = N(r)$ (not necessarily monotonically increasing as a function of the radius r), then there also exists a monotonically increasing solution $\acute{N} = \acute{N}(r)$.*

SKETCHED PROOF: Lemma 8.3 is basically the observation that the integration variable $x \equiv \ln r$ only enters implicitly via the function $N = N(x)$, and that the Lebesgue measure $\mathrm{d}x$ is translation invariant. □

From now on we can and we will make the following assumption 8.4 without loss of generality.

Assumption 8.4 *The solution $N = N(r)$ is a monotonically increasing function of r.*

At this point, we introduce a technical assumption 8.5 in order to proceed.

Assumption 8.5 *The inverse solution $r = r(N)$ exists and is differentiable with Lebesgue measurable derivative.*

The Assumption 8.5 implies that one can define a Lebesgue measurable density

$$\rho(N) \;:=\; \tfrac{\mathrm{d}\ln r(N)}{\mathrm{d}\ln N} \;\geq\; 0 \;. \tag{39}$$

Let us call the definition domain of the inverse solution $r = r(N)$ for $[N_*, N_m]$. In other words, $r(N_*) = r_*$ and $r(N_m) = R$.

Lemma 8.6 (Reformulation in terms of test functions) *Under the assumptions 8.4-8.5, the integral equation (31) becomes equivalent to*

$$\boxed{\forall \eta \in C_c^\infty((0,\infty)): \quad \int_{N_*}^{N_m} \rho(N)\mathrm{d}N \; \tfrac{\mathrm{d}\eta(N)}{\mathrm{d}N} \;=\; -\eta(1) \;.} \tag{40}$$

REMARK: Here $C_c^\infty((0,\infty))$ denotes the set of infinitely often differentiable functions η defined on the open interval $(0,\infty)$, and such that η has compact support in $(0,\infty)$. Compact support means that the function η is assumed to vanish identically in whole neighbourhoods around of $N = 0$ and $N = \infty$. It is therefore natural to extend η smoothly to the closed interval $[0,\infty]$ by assigning to η the values $\eta(0) = 0 = \eta(\infty)$ at the end points $N = 0$ and $N = \infty$.

PROOF: When we substitute the inverse solution $r = r(N)$, equation (37) becomes

$$e^{L^2} \;=\; \left(1 + \tfrac{\mathrm{d}}{\mathrm{d}\alpha}\right) \int_{N_*}^{N_m} \rho(N) \tfrac{\mathrm{d}N}{N^2} \exp\left[(\tfrac{\alpha L}{N})^2\right]\Big|_{\alpha=1} \;. \tag{41}$$

Next perform the elementary substitution $\nu \equiv 1/N$ with limits $\nu_m \equiv 1/N_m$, and $\nu_* \equiv 1/N_*$. Furthermore, multiply both sides with $e^{-(L\mu)^2}$, where $\mu > 0$ is a positive parameter. Then

$$e^{L^2(1-\mu^2)} \;=\; \left(1 + \tfrac{\mathrm{d}}{\mathrm{d}\alpha}\right) \int_{\nu_m}^{\nu_*} \rho(\nu)\mathrm{d}\nu \; e^{L^2((\alpha\nu)^2-\mu^2)}\Big|_{\alpha=1} \;. \tag{42}$$

Recall that the Dirac delta distribution $\delta(x)$ has the Fourier integral representation $\delta(x) = \int_{-\infty}^{\infty} \frac{\mathrm{d}p}{2\pi} e^{\mathrm{i}px}$. By integrating $L^2 \;=\; \mathrm{i}p$ along the imaginary axis in Eq. (42), one gets

$$\delta(1-\mu^2) \;=\; \left(1 + \tfrac{\mathrm{d}}{\mathrm{d}\alpha}\right) \int_{\nu_m}^{\nu_*} \rho(\nu)\mathrm{d}\nu \; \delta((\alpha\nu)^2 - \mu^2)\Big|_{\alpha=1} \;. \tag{43}$$

By using the Jacobian formula for the Dirac delta distribution

$$\delta(f(x)) \;=\; \sum_{\substack{x_0 \\ f(x_0)=0}} \tfrac{1}{|f'(x_0)|} \; \delta(x - x_0) \;, \tag{44}$$

and multiplying both sides with 2, one gets

$$\delta(\mu-1) \;=\; \left(1+\tfrac{\mathrm{d}}{\mathrm{d}\alpha}\right)\int_{\nu_m}^{\nu_*}\rho(\nu)\mathrm{d}\nu\;\tfrac{1}{\mu}\delta(\alpha\nu-\mu)\Big|_{\alpha=1}\;, \tag{45}$$

where we have assumed that $\mu > 0$ is positive. Thus for a test function $\eta \in C_c^\infty((0,\infty))$, one calculates

$$\begin{aligned}\eta(1) &= \int_0^\infty \mathrm{d}\mu\;\eta(\mu)\delta(\mu-1) \overset{(45)}{=} \left(1+\tfrac{\mathrm{d}}{\mathrm{d}\alpha}\right)\int_{\nu_m}^{\nu_*}\rho(\nu)\mathrm{d}\nu\int_0^\infty \mathrm{d}\mu\;\tfrac{\eta(\mu)}{\mu}\delta(\alpha\nu-\mu)\Big|_{\alpha=1}\\ &= \left(1+\tfrac{\mathrm{d}}{\mathrm{d}\alpha}\right)\int_{\nu_m}^{\nu_*}\rho(\nu)\mathrm{d}\nu\;\tfrac{\eta(\alpha\nu)}{\alpha\nu}\Big|_{\alpha=1} \;=\; \int_{\nu_m}^{\nu_*}\rho(\nu)\mathrm{d}\nu\left[\tfrac{\eta(\alpha\nu)}{\alpha\nu}-\tfrac{\eta(\alpha\nu)}{\alpha^2\nu}+\tfrac{\eta'(\alpha\nu)}{\alpha}\right]\Big|_{\alpha=1}\\ &= \int_{\nu_m}^{\nu_*}\rho(\nu)\mathrm{d}\nu\tfrac{\mathrm{d}\eta(\nu)}{\mathrm{d}\nu}\;.\end{aligned} \tag{46}$$

Now translate (46) back to the $N \equiv 1/\nu$ variable to obtain Eq. (40). □

Lemma 8.7 *Eq. (40) has no solutions for ρ that respects the bounds (32) on N.*

PROOF: The Fundamental Lemma of calculus of variation (in the strengthen version of du Bois-Reymond) [22] shows that ρ must be a constant up to contributions that vanish almost everywhere. (In particular, we stress that it is not enough for ρ to be only piecewise constant.) Thus one may pull the density ρ outside of the integral (40), and integrate to get

$$\forall\eta\in C_c^\infty((0,\infty)):\quad \rho\left(\eta(N_m)-\eta(N_*)\right) \;=\; -\eta(1)\;. \tag{47}$$

Collapsing limits $N_* = N_m$ are clearly not a solution. Assuming $N_* < N_m$, equation (47) has two solutions, $(\rho=1, N_*=1, N_m=\infty)$, or $(\rho=-1, N_*=0, N_m=1)$. However, none of these two solutions respect the bounds (32) on N, and the latter is actually monotonically decreasing. □

References

[1] Pendry J B 2000 Phys. Rev. Lett. **85** 3966

[2] Soukoulis C M, Linden S and Wegener M 2007 Science **315** 47

[3] Fang N *et al* 2005 Science **308** 534

[4] Stockman M I 2007 Phys. Rev. Lett. **98** 177404

[5] Leonhardt U 2009 New J. Phys. **11** 093040

[6] Leonhardt U and Philbin T G 2010 Phys. Rev. A **81** 011804(R)

[7] Ma Y G *et al* 2011 New J. Phys. **13** 033016

[8] Maxwell J C 1854 Camb. Dublin Math. J. **8** 188

[9] Born M and Wolf E 2006 *Principles of optics* (Cambridge: Cambridge University Press)

[10] Hendi A, Henn J and Leonhardt U 2006 Phys. Rev. Lett **97** 073902

[11] Leonhardt U and Philbin T 2010 *Geometry and Light: The Science of Invisibility* (Dover: Mineola)

[12] Firsov O B 1953 Zh. Eksp. Teor. Fiz. **24**, 279

[13] Luneburg R K 1964 *Mathematical Theory of Optics* (Berkeley: University of California Press)

[14] Ostrovsky V N 1997 Phys. Rev. A **56** 526

[15] Landau L D and Lifshitz E M 1976 *Mechanics* (Oxford: Butterworth-Heinemann)

[16] Demkov Y N and Ostrovsky V N 1971 Sov. Phys.-JETP **33** 1083

[17] Eaton J E 1952 Trans. IRE Ant. Prop. **4** 66

[18] Mi nano J C 2006 Opt. Express **14** 9627

[19] Tyc T and Šarbort M 2010 arXiv:1010.3178

[20] Tyc T 2011 arXiv:1103.3406

[21] Rudin W 1966 *Real and complex analysis* (New York: McGraw-Hill)

[22] Hörmander L 1990 *The Analysis of Linear Partial Differential Operators I, (Distribution theory and Fourier Analysis)* (Springer-Verlag)